

Discussion of Different Model Approaches for the Flow Behavior of Ice

Julia Christmann^{1,*}, Martin Rückamp², Ralf Müller¹, and Angelika Humbert^{2,3}

¹ Institute of Applied Mechanics, University of Kaiserslautern

² Section of Glaciology, Alfred-Wegener-Institut Helmholtz Zentrum für Polar- und Meeresforschung, Bremerhaven

³ Department of Geosciences, University of Bremen

Ice of Antarctic ice shelves is assumed to behave on long-term as an incompressible viscous fluid, which is dominated on short time scales by the elastic response. Hence, a viscoelastic material model is required. The thermodynamic pressure is treated differently in elastic and viscous models. For small deformations, the elastic isometric stress for $\nu \rightarrow 0.5$ gives similar results to those solving for pressure in an incompressible laminar flow model. A viscous model, in which the thermodynamic pressure is approximated by an elastic isometric stress, can be easily extended to viscoelasticity.

© 2016 Wiley-VCH Verlag GmbH & Co. KGaA, Weinheim

1 Introduction

Ice shelves are floating extensions of ice streams and glaciers. The mass loss of ice shelves at the ice front is called calving. The understanding of calving processes requires to investigate the stress at the ice front, see [1]. Here, different approaches are compared to deal with the pressure term in modeling the stress situation of ice shelves.

In an “infinitely” wide ice shelf, it is sufficient to model a 2-D geometry assuming plane strain conditions. The dimensions and boundary conditions are given in Fig. 1 with the displacement vector $\mathbf{u} = (u, w)^T$. The traction at the bottom balances the weight of the ice shelf. Hence, this traction condition and the one at the ice front (right side) are given by the Robin-type boundary condition $\sigma_n = \rho_{sw}g(-z - w)$ for $-z - w < 0$. The Cartesian coordinate z originates at sea level and $\rho_{sw} = 1028 \frac{\text{kg}}{\text{m}^3}$ is the density of sea water.

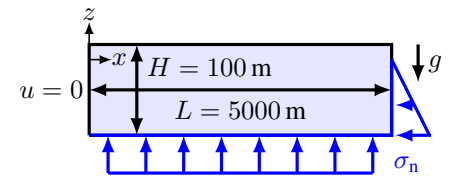


Fig. 1: Boundary conditions.

2 Linear Viscosity

In the incompressible laminar flow module of the commercial finite element software COMSOL*, the quasi-static momentum balance is solved using the incompressibility condition, the linearized kinematic relation and the linear viscous material law

$$\text{div } \boldsymbol{\sigma} + \mathbf{f} = \mathbf{0}, \quad \text{div } \mathbf{v} = 0, \quad \dot{\boldsymbol{\varepsilon}} = \frac{1}{2} (\text{grad } \mathbf{v} + (\text{grad } \mathbf{v})^T), \quad \boldsymbol{\sigma} = -p\mathbf{I} + \boldsymbol{\sigma}^D \quad \text{with } \boldsymbol{\sigma}^D = 2\eta\dot{\boldsymbol{\varepsilon}}. \quad (1)$$

The Cauchy stress tensor is denoted by $\boldsymbol{\sigma}$ with its deviator $\boldsymbol{\sigma}^D$ and $\dot{\boldsymbol{\varepsilon}}$ is the strain rate tensor. The volume forces \mathbf{f} consists of the ice weight $f_z = -\rho_{ice}g$ with the ice density $\rho_{ice} = 910 \frac{\text{kg}}{\text{m}^3}$ and $\eta = 10^{15} \text{ Pa s}$ is the viscosity, both common values for ice. This model has the velocities \mathbf{v} and the fluid pressure p as unknowns (Q2P1 elements). Additionally, the computational domain is adapted in every time step by a moving mesh, which also includes an accumulation rate of $0.35 \frac{\text{m}}{\text{a}}$. This laminar flow model is compared to a viscous model, which approximates the thermodynamic pressure by an elastic isometric stress described by a constitutive relation

$$\text{div } \boldsymbol{\sigma} + \mathbf{f} = \mathbf{0}, \quad \boldsymbol{\varepsilon} = \frac{1}{2} (\text{grad } \mathbf{u} + (\text{grad } \mathbf{u})^T), \quad \boldsymbol{\sigma} = K \text{tr}(\boldsymbol{\varepsilon})\mathbf{I} + \boldsymbol{\sigma}^D \quad \text{with } \boldsymbol{\sigma}^D = 2\eta\dot{\boldsymbol{\varepsilon}} \quad (2)$$

as suggested in [2]. The displacement vector \mathbf{u} contains the unknowns in this model and $K = \frac{E}{3(1-2\nu)}$ is the bulk modulus including the elastic parameters, namely Young’s modulus E and Poisson’s ratio ν . Hence, the changes of volume are reversible based on the fundamental assumption that the volume-changing part of the stress tensor is purely elastic. Thus the viscous material is only characterized by the stress deviator. Adapting the deviatoric stress, it is easily possible to expand this model to viscoelasticity, which is required to describe the behavior of ice [3]. In order to include the short-term elastic behavior, which is often assumed to be brittle and compressible for ice [4], the compressibility is only included in the elastic part.

3 Results

In the following, the analysis of the expression $\frac{1}{3}\text{tr}(\boldsymbol{\sigma})$, the volumetric part of the stress tensor, shows the application field approximating the thermodynamic pressure by the elastic isometric stress. For the latter case, Poisson’s ratio ν has to converge to 0.5 to simulate incompressibility and Young’s modulus is $E = 9 \text{ GPa}$, a common value assumed for polycrystalline ice [4].

* Corresponding author: e-mail jchristm@rhrk.uni-kl.de, phone +49 631 205 2126, fax +49 631 205 2128

* www.comsol.com

Figure 2 illustrates the thermodynamic pressure a), the elastic isometric stress b) and the difference of both c) in the ice shelf after one year. The difference is at least two order of magnitude smaller than the pressure. The major deviations occur directly at the ice front. These variations are the result of the computation on different configurations. In the laminar flow module, the model uses the external and internal forces with regard to the current configuration based on the moving mesh. However, the viscous model computes the actual displacements, whereas the applied forces act on the reference configuration.

Calving processes of ice shelves are controlled by the first (most tensile) principal stress. It is therefore essential to consider the stress distribution at the upper surface in more detail as the largest tensile stress is located on this surface. The tensile stress in the upper part is caused by the bending moment of the boundary disturbance at the ice front. Figure 3 shows the volumetric part of the stress tensor over the dimensionless distance to the ice front at the upper surface. In this figure, the solid lines depict the stress distribution using the elastic isometric approach and the dashed lines display the thermodynamic pressure. The blue curves after 7 days are nearly identical. Also the red curves, which shows the stress result after one year, are close together and it is sufficient to take the elastic isometric stress as a good approximation of the thermodynamic pressure. However, the deviation gets larger with an increase of the simulation time. After 10 years, the difference is already noticeable with a shift of maximal 1200 Pa. This deviation originates from the above mentioned computation using different configurations and the additional accumulation rate of the laminar flow model. In order to illustrate this, the deflection at the upper surface is shown in Fig. 4 for the same points in time. The deflections of the two models differ after $t = 10$ a and lead to the stress deviation.

Figure 5 points out that the elastic isometric stress curves converge to the thermodynamic pressure for $\nu \rightarrow 0.5$ and $t = 7$ d. A Poisson's ratio of a compressible material, see the gray curve with $\nu = 0.3$, gives a similar maximum of the volumetric stress, which is caused by the boundary disturbance at the ice front. However, the remaining stress distribution differs considerably from the incompressible case. The thermodynamic pressure is very well approximated by the isometric elastic stress taking $\nu = 0.49$. The approximation quality is also slightly dependent on Young's modulus E as this value influences the bulk modulus K . Decreasing E below a certain value means that Poisson's ratio of $\nu = 0.499$ is needed to provide sufficient results.

4 Conclusion

In the case of small deformation on short time scales, like days to months, the thermodynamic pressure of the incompressible laminar flow model is very well approximated by the elastic isometric stress for $\nu \rightarrow 0.5$. Stress distributions using finite deformations have to be considered for longer simulation times.

Acknowledgements This work was supported by DFG priority program SPP 1158, project numbers HU 1570/5-1; MU 1370/7-1. Discussion with Dietmar Gross (TU Darmstadt) is gratefully acknowledged.

References

- [1] J. Christmann, C. Plate, R. Müller, and A. Humbert: Viscous and Viscoelastic Stress States at the Calving Front of Antarctic Ice Shelves, *Annals of Glaciology*, 2016.
- [2] Darby, R.: Viscoelastic fluids: an introduction to their properties and behavior, M. Dekker, New York, 1976.
- [3] Gudmundsson, G. H.: Ice-stream response to ocean tides and the form of the basal sliding law, *The Cryosphere*, Vol. 5, 259-270, 2011.
- [4] M. A. Rist, P. R. Sammonds, S. A. F. Murrell, P. G. Meredith, C. S. M. Doake, and K. Matsuki, Experimental and theoretical fracture mechanics applied to Antarctic ice fracture and surface crevassing, *Journal of Geophysical Research*, Vol. 104(B2), 2973–2987, 1999.

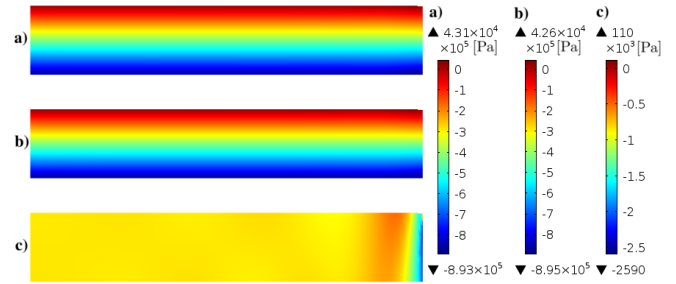


Fig. 2: Comparison ($t = 1$ a, $\nu = 0.499$) of a) thermodynamic pressure $-p$, b) elastic isometric stress $K \text{tr}(\epsilon)$, c) difference $K \text{tr}(\epsilon) + p$.

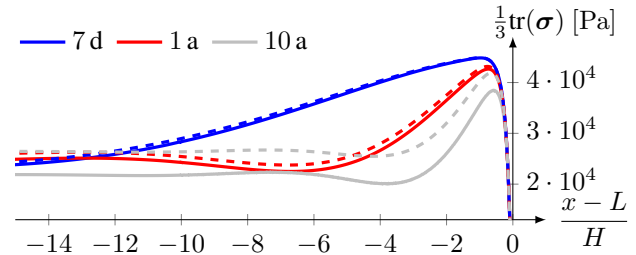


Fig. 3: Stress distribution after the upper surface using $K \text{tr}(\epsilon)$ and $\nu = 0.499$ (solid lines) instead of $-p$ (dashed lines).

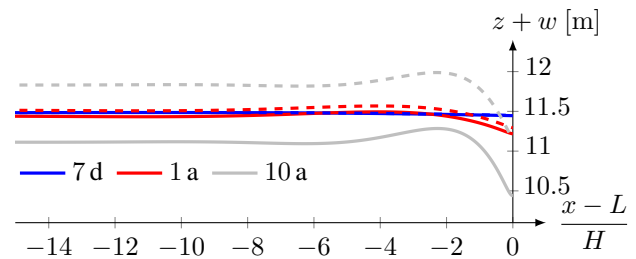


Fig. 4: Deflection w of the upper surface for $\nu = 0.499$.

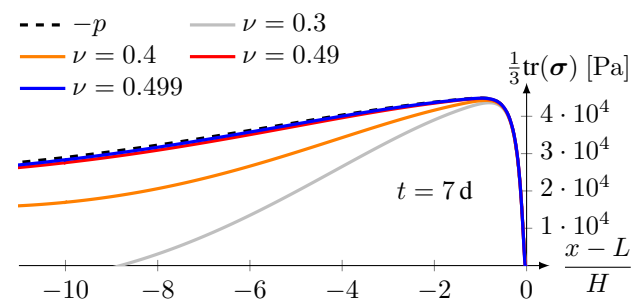


Fig. 5: Stress distribution for different values of Poisson's ratio.